Group 2 Red: Non-minimally Coupled Higgs-like Model / Induced-Gravity Limit

Gravitational Baryogenesis in Scalar-Tensor Gravity (Red STT-2)

Arsh Dhawan, Subhas Hegde, Atrajit Roy Chaudhuri

July 2026

Contents

1 Basics

The common Jordan-frame scalar-tensor action is

$$S_J = \int d^4x\sqrt{-g}\left[\frac{1}{2}F(\varphi)R - \frac{1}{2}K(\varphi)\nabla_\mu\varphi\nabla^\mu\varphi - U(\varphi)\right] + S_m[g_{\mu\nu},\psi]. \tag{1}$$

The scalar-tensor thermodynamic variable to track is

$$KT = \frac{|\dot{F}|}{8\pi F} = \frac{|F_{,\varphi}\dot{\varphi}|}{8\pi F}. \tag{2}$$

This is the effective gravitational temperature-conductivity product. The GR limit is

$$F \to F_0 = \text{constant}, \qquad KT \to 0. \tag{3}$$

Heating means that the scalar-tensor sector moves toward larger KT, while cooling means that it relaxes toward the GR equilibrium state $KT = 0$. Here $KT = 0$ is the thermal equilibrium indicator; full dynamical recovery of GR also requires negligible scalar backreaction.

For scalar-tensor baryogenesis, we use a derivative current interaction of the form

$$\mathcal{L}_{\rm int} = \frac{1}{M_*^d}\nabla_\mu\mathcal{I}(\varphi)J^\mu_{B-L}, \qquad \mu_{B-L} = \frac{\dot{\mathcal{I}}}{M_*^d}. \tag{4}$$

Here $d = [\mathcal{I}]$, so $d = 1$ for $\mathcal{I} = \varphi$ and $d = 2$ for $\mathcal{I} = M_{\rm Pl}^2\ln(F/M_{\rm Pl}^2)$. The interaction is physically operative while $B-L$-violating reactions are active. A particularly convenient thermodynamic choice is

$$\mathcal{I}(\varphi) = M_{\rm Pl}^2\ln\left(\frac{F(\varphi)}{M_{\rm Pl}^2}\right), \tag{5}$$

for which

$$\dot{\mathcal{I}} = M_{\rm Pl}^2\frac{\dot{F}}{F} = 8\pi M_{\rm Pl}^2\epsilon_F\, KT, \qquad \epsilon_F = \operatorname{sign}(\dot{F}). \tag{6}$$

This makes the baryogenesis chemical potential directly proportional to the scalar-tensor thermodynamic departure from GR.

We can also use the "natural" case $\mathcal{I}(\varphi) = \varphi$, for which

$$|\dot{\varphi}| = 8\pi F\,\frac{KT}{|F_{,\varphi}|}, \tag{7}$$

so the generated asymmetry depends directly on KT, F, and $F_{,\varphi}$. The sign of $\dot{\varphi}$ must be tracked separately.

2 The Model: Red STT-2

2.1 Jordan-frame model

We take the Jordan-frame model of Non-minimally Coupled Higgs-like type,

$$F(\varphi) = M_0^2 + \xi\varphi^2, \qquad K(\varphi) = 1, \tag{8}$$

with

$$U(\varphi) = \frac{\lambda}{4}\left(\varphi^2 - v^2\right)^2 + U_0. \tag{9}$$

The field φ plays the role of a Higgs-like scalar with two degenerate true vacua at $\varphi = \pm v$ and an unstable symmetric extremum at $\varphi = 0$; M_0^2 is a bare (possibly zero, in the pure induced-gravity limit) Planck mass, and ξ is the non-minimal coupling. Then

$$F_{,\varphi} = 2\xi\varphi, \qquad F_{,\varphi\varphi} = 2\xi, \qquad U_{,\varphi}(\varphi) = \lambda\varphi\left(\varphi^2 - v^2\right), \qquad U_{,\varphi\varphi}(\varphi) = \lambda\left(3\varphi^2 - v^2\right), \tag{10}$$

and, directly from the general definition,[1]

$$KT = \frac{|F_{,\varphi}\dot{\varphi}|}{8\pi F} = \frac{|\xi\varphi\dot{\varphi}|}{4\pi(M_0^2 + \xi\varphi^2)}. \tag{11}$$

For baryogenesis coupling, we use either

$$\mathcal{I}(\varphi) = \frac{\varphi^2}{M_{\rm Pl}}, \tag{12}$$

or the thermodynamic choice

$$\mathcal{I}(\varphi) = M_{\rm Pl}^2 \ln\left(\frac{M_0^2 + \xi\varphi^2}{M_{\rm Pl}^2}\right). \tag{13}$$

the burst of KT is triggered by a *field-space* phase transition – the relaxation of φ from the unstable symmetric point $\varphi = 0$ toward the true vacuum $\varphi = \pm v$, in close analogy with electroweak symmetry breaking.

3 Task 1: Complete Field Equations and FLRW Reduction

3.1 General metric and scalar field equations

Varying S_J with respect to $g^{\mu\nu}$ gives the Jordan-frame metric field equation

$$FG_{\mu\nu} = T_{\mu\nu} + K\left(\nabla_\mu\varphi\nabla_\nu\varphi - \frac{1}{2}g_{\mu\nu}\nabla_\rho\varphi\nabla^\rho\varphi\right) - Ug_{\mu\nu} + \nabla_\mu\nabla_\nu F - g_{\mu\nu}\Box F, \tag{14}$$

where $T_{\mu\nu} \equiv -\frac{2}{\sqrt{-g}}\delta S_m/\delta g^{\mu\nu}$ is the matter stress tensor. Varying with respect to φ (with $K = 1$ constant, so $K_{,\varphi} = 0$) gives, after one integration by parts on the kinetic term,

$$\Box\varphi + \frac{1}{2}F_{,\varphi}R - U_{,\varphi} = 0. \tag{15}$$

3.2 FLRW background quantities

We use the flat FLRW metric $ds^2 = -dt^2 + a^2(t)\delta_{ij}dx^i dx^j$, for which

$$G_{00} = 3H^2, \qquad G_{ij} = -\left(2\dot{H} + 3H^2\right)g_{ij}, \qquad R = 6\left(\dot{H} + 2H^2\right), \tag{16}$$

and, for a homogeneous scalar $\varphi = \varphi(t)$,

$$\nabla_\mu\varphi\nabla^\mu\varphi = -\dot{\varphi}^2, \qquad \nabla_0\nabla_0 F = \ddot{F}, \qquad \Box F = -\ddot{F} - 3H\dot{F}, \qquad \nabla_i\nabla_j F - g_{ij}\Box F = g_{ij}\left(\ddot{F} + 2H\dot{F}\right). \tag{17}$$

Matter is taken as a perfect fluid, $T_{\mu\nu} = (\rho_m + p_m)u_\mu u_\nu + p_m g_{\mu\nu}$.

[1] A good particle physicist would have taken planck Mass as 1. My MS advisor would be disappointed in me *Insert-sad-emoji -here.*

3.3 Deriving the First Friedmann equation

The kinetic term in Eq. (14) projects onto the $(0,0)$ component as

$$K\left(\dot{\varphi}^2 - \tfrac{1}{2}g_{00}(-\dot{\varphi}^2)\right) = \tfrac{1}{2}K\dot{\varphi}^2, \tag{18}$$

using $g_{00} = -1$. The potential term gives $-Ug_{00} = U$, and the non-minimal derivative term gives $\nabla_0\nabla_0 F - g_{00}\Box F = \ddot{F} + \Box F = \ddot{F} + (-\ddot{F} - 3H\dot{F}) = -3H\dot{F}$.
Using all this, the $(0,0)$ component of Eq. (14) gives us

$$3FH^2 = \rho_m + \frac{1}{2}K\dot{\varphi}^2 + U - 3H\dot{F}. \tag{19}$$

Substituting $F = M_0^2 + \xi\varphi^2$, $K = 1$, $U = \frac{\lambda}{4}(\varphi^2 - v^2)^2 + U_0$ and $\dot{F} = 2\xi\varphi\dot{\varphi}$, the **First Friedmann equation** for this model comes out to be

$$\boxed{3\left(M_0^2 + \xi\varphi^2\right)H^2 = \rho_m + \frac{1}{2}\dot{\varphi}^2 + \frac{\lambda}{4}\left(\varphi^2 - v^2\right)^2 + U_0 - 6H\xi\varphi\dot{\varphi}.} \tag{20}$$

3.4 Deriving the Second Friedmann equation

If we consider the spatial (i,j) component of Eq. (14) and make sure to divide out g_{ij}, we get

$$-F\left(2\dot{H} + 3H^2\right) = p_m + \frac{1}{2}K\dot{\varphi}^2 - U + \ddot{F} + 2H\dot{F}. \tag{21}$$

Now we can use (19) to eliminate the $3FH^2$ term,

$$-2F\dot{H} = \left[\rho_m + \frac{1}{2}K\dot{\varphi}^2 + U - 3H\dot{F}\right] + p_m + \frac{1}{2}K\dot{\varphi}^2 - U + \ddot{F} + 2H\dot{F}, \tag{22}$$

giving us the second Friedmann equation;

$$-2F\dot{H} = \rho_m + p_m + K\dot{\varphi}^2 + \ddot{F} - H\dot{F}. \tag{23}$$

Using $\dot{F} = 2\xi\varphi\dot{\varphi}$ and $\ddot{F} = 2\xi\dot{\varphi}^2 + 2\xi\varphi\ddot{\varphi}$, this reduces to

$$\boxed{-2\left(M_0^2 + \xi\varphi^2\right)\dot{H} = \rho_m + p_m + (1+2\xi)\dot{\varphi}^2 + 2\xi\varphi\ddot{\varphi} - 2H\xi\varphi\dot{\varphi}.} \tag{24}$$

3.5 Scalar (Klein–Gordon–like) field equation

Using $\Box\varphi = -\ddot{\varphi} - 3H\dot{\varphi}$ in Eq. (15) and $F_{,\varphi} = 2\xi\varphi$ gives, in FLRW,

$$\boxed{\ddot{\varphi} + 3H\dot{\varphi} - \xi\varphi R + \lambda\varphi\left(\varphi^2 - v^2\right) = 0, \qquad R = 6\left(\dot{H} + 2H^2\right).} \tag{25}$$

This is the standard non-minimally coupled Klein–Gordon equation. [2]

[2] Note how the field feels both the usual quartic force and an effective curvature-dependent mass term $-\xi R\varphi$, which is the gravitational analogue of a finite-temperature/curvature correction to the Higgs potential. An interesting observation!

3.6 Trace equation

Taking the trace of Eq. (14) with $g^{\mu\nu}G_{\mu\nu} = -R$ gives

$$FR = -T^{(m)} + K\nabla_\rho\varphi\nabla^\rho\varphi + 4U + 3\Box F = -T^{(m)} - \dot{\varphi}^2 + 4U - 3\ddot{F} - 9H\dot{F}, \tag{26}$$

with $T^{(m)} = g^{\mu\nu}T^{(m)}_{\mu\nu} = -\rho_m + 3p_m$. Substituting $T^{(m)} = -\Delta\rho_m$ with $\Delta \equiv 1 - 3w$ ($w = p_m/\rho_m$), Eq. (26) shows that, unlike in pure $f(R)$ gravity, R receives a contribution from both the matter trace but and also the scalar's own potential energy $4U$. In particular, even for an idealised conformal radiation fluid ($\Delta = 0$) with the field sitting at rest at its potential minimum ($\dot{\varphi} = \ddot{\varphi} = 0$), Eq. (26) gives $FR = 4U(v) = 4U_0$: a nonzero residual vacuum energy U_0 sources curvature on its own, exactly like a small cosmological constant. This is used in the following section/task too.

3.7 Matter continuity and system closure

Matter is minimally coupled to $g_{\mu\nu}$, so the usual conservation law holds independently of F and K:

$$\dot{\rho}_m + 3H(\rho_m + p_m) = 0. \tag{27}$$

In case of radiation, since $p_m = \frac{1}{3}\rho_m$, so $\rho_m \propto a^{-4}$ in the absence of scalar backreaction.

3.8 Thermodynamic order parameter KT

As shown in Eq. (11),

$$KT \equiv \frac{|\dot{F}|}{8\pi F} = \frac{|\xi\varphi\dot{\varphi}|}{4\pi\left(M_0^2 + \xi\varphi^2\right)}. \tag{28}$$

KT becomes 0 exactly at $\varphi = 0$ (only when $\dot{\varphi} = 0$ at that point, since $\varphi = 0$ makes the prefactor vanish but not necessarily $\dot{\varphi}$) and at any fixed point $\dot{\varphi} = 0$, including both vacuum $\varphi = \pm v$.
$KT \to 0$ as the field settles into either true vacuum, recovering GR with an effective Planck mass $F_* \equiv M_0^2 + \xi v^2$.

3.8.1 Heating/cooling rate

For later use in the $(\dot{KT})$ root analysis of Task 4, lets jut do the rate of change of KT for this model. Writing the signed variable $X_F \equiv \dot{F}/(8\pi F)$, so that $KT = |X_F|$ and $\epsilon_F = \operatorname{sign}(X_F) = \operatorname{sign}(\dot{F})$,

$$\frac{d(KT)}{dt} = \epsilon_F\dot{X}_F = \epsilon_F\left[\frac{\ddot{F}}{8\pi F} - 8\pi(KT)^2\right], \tag{29}$$

using $\dot{F}/F = 8\pi\epsilon_F KT$. For the given model, $\ddot{F} = 2\xi\dot{\varphi}^2 + 2\xi\varphi\ddot{\varphi}$, and $\ddot{\varphi}$ is fixed by the scalar equation (25), so

$$\frac{d(KT)}{dt} = \epsilon_F\left\{\frac{2\xi\dot{\varphi}^2 + 2\xi\varphi\left[-3H\dot{\varphi} + \xi\varphi R - \lambda\varphi(\varphi^2 - v^2)\right]}{8\pi\left(M_0^2 + \xi\varphi^2\right)} - 8\pi(KT)^2\right\}. \tag{30}$$

This is the Riccati-type evolution equation for this model's KT, containing a self-heating term $-8\pi(KT)^2$ (always cooling, with our sign convention, since it enters with an overall minus sign multiplying ϵ_F times a positive quantity – ie its sign must be examined together with ϵ_F, as told in Task 4), a Hubble-friction term $\propto -3H\dot{\varphi}\varphi$, a curvature-driven term $\propto \xi\varphi^2 R$, and a potential-driven term $\propto -\lambda\varphi^2(\varphi^2 - v^2)$. Equation (30) is exactly the one whose roots (as a function of KT, at fixed φ, H, R) will be analyzed in Task 4, it is quoted here to make connection between T1 and T4 and showing that T1 provides everything (φ, $\dot{\varphi}$, R, H) that Task 4 needs.

3.9 Viability and stability constraints

Two structural conditions must be applied on the field range.

Condition 1 ($F > 0$, correct-sign gravity). For $\xi \geq 0$ and $M_0^2 \geq 0$, $F = M_0^2 + \xi\varphi^2 > 0$ for all φ. For $\xi < 0$, F changes sign at

$$|\varphi| = \varphi_c \equiv \frac{M_0}{\sqrt{|\xi|}}, \tag{31}$$

so a negative non-minimal coupling is only viable on the restricted domain $|\varphi| < \varphi_c$; in particular the true vacuum must satisfy $v < \varphi_c$, i.e. $|\xi|v^2 < M_0^2$.

Condition 2 (no ghost). Eliminating R between the scalar equation and the trace equation gives, for a general Jordan-frame model, an effective kinetic coefficient $2KF + 3F_{,\varphi}^2$ that must stay positive. For this model,

$$2KF + 3F_{,\varphi}^2 = 2\left(M_0^2 + \xi\varphi^2\right) + 3(2\xi\varphi)^2 = 2M_0^2 + 2\xi\varphi^2\left(1 + 6\xi\right). \tag{32}$$

For $\xi \geq 0$ this is positive for all φ (as $M_0^2 \geq 0$). For $-1/6 \leq \xi < 0$ it decreases with $|\varphi|$ but, considering at the sign-change point $\varphi = \varphi_c$ where $F = 0$, it equals $12\xi^2 M_0^2 > 0$; the binding constraint thus remains same as Condition 1, $|\varphi| < \varphi_c$. For $\xi < -1/6$ the coefficient $(1 + 6\xi)$ is negative, so the term $2\xi\varphi^2(1 + 6\xi)$ is a product of two negative factors and thus positive, and the no-ghost condition is satisfied throughout the whole $F > 0$ domain.
In all cases studied in this project ($\xi > 0$, as in Higgs inflation and induced gravity, where ξ can range from order $\mathcal{O}(1)$ up to the order $\xi \sim 10^4$) ie both of the conditions hold trivially for every field value, and the special values $\xi = 0$ (minimal coupling), $\xi = 1/6$ (conformal coupling in four dimensions) and $\xi \gg 1$ (Higgs-inflation/induced-gravity limit) are all continuously connected in the parameter space.

4 Task 2: Radiation-Era Solutions

4.1 Problems in deriving a universal closed-form solution

The coupled system, Eqs. (20), (24) and (25), does not admit a single closed-form solution valid across the whole cosmological history. The obstruction here is structurally different from the essential (transcendental) singularity found in exponential $f(R)$ gravity. In this case it is the *cubic* nonlinearity $\lambda\varphi^3$ in $U_{,\varphi}$, combined with the two-way feedback between φ and $R = 6(\dot{H} + 2H^2)$ through Eq. (20)–(24), that prevents a generic power-law ansatz $a(t) \propto t^p$ from solving the scalar equation exactly for arbitrary field amplitude.
Direct, exact or controlled-approximation solutions do exist(below), all of which are directly usable for the baryongenesis calculation of Task 3.

4.2 Exact fixed points

If the field sits exactly at rest at an extremum of U, i.e. $\varphi = \varphi_* = \{0, \pm v\}$ with $\dot{\varphi} = \ddot{\varphi} = 0$, the scalar equation (25) requires

$$-\xi\varphi_* R + \lambda\varphi_*\left(\varphi_*^2 - v^2\right) = 0. \tag{33}$$

At $\varphi_* = \pm v$ this is satisfied identically for any R only if $\xi = 0$
On the other hand, for $\xi \neq 0$ it is satisfied exactly only when $R = 0$, i.e. in the idealized conformal-radiation limit (see Sec. 4.5 below with $U_0 = 0$). In that idealized limit,

$$\varphi(t) = \pm v = \text{const}, \qquad F(t) = F_* \equiv M_0^2 + \xi v^2 = \text{const}, \qquad KT = 0. \tag{34}$$

This is the GR-equilibrium fixed point of the model, an effective Newton's constant $G_{\rm eff} = 1/(8\pi F_*)$, with the scalar-tensor sector having no effect. It carries no CP-violating source and cannot by itself generate an asymmetry – exactly the same sterile role played by the $R = 0$ fixed point in the exponential-gravity project. The extremum $\varphi_* = 0$ is likewise an exact (but linearly unstable, see below) fixed point of the same type.

4.3 Small oscillations about the true vacuum(After transition)

Consider $\varphi(t) = v + \delta\varphi(t)$ with $|\delta\varphi| \ll v$, in the region where scalar back-reaction on the background is negligible (spectator condition, $\rho_\varphi \ll \rho_r$), so that $H(t) \simeq 1/(2t)$ follows the ordinary GR radiation solution and hence, using perfect raditation field limit on R , $R \simeq 0$ to leading order. Linearizing Eq. (25) about $\varphi = v$, with $U_{,\varphi\varphi}(v) = 2\lambda v^2 \equiv m_h^2$ (the familiar Higgs-mass relation $m_h^2 = 2\lambda v^2$), gives

$$\ddot{\delta\varphi} + \frac{3}{2t}\dot{\delta\varphi} + m_h^2\,\delta\varphi \simeq 0. \tag{35}$$

Derivation. Substituting $\delta\varphi(t) = t^{-1/4}u(t)$ into Eq. (35) and multiplying through by $t^{1/4}$ gives,

$$\ddot{u} + \frac{1}{t}\dot{u} + \left(m_h^2 - \frac{1}{16t^2}\right)u = 0, \tag{36}$$

which is exactly Bessel's equation of order $\nu = 1/4$ in the variable $m_h t$. Hence the exact solution is

$$\delta\varphi(t) = t^{-1/4}\left[C_1 J_{1/4}(m_h t) + C_2 Y_{1/4}(m_h t)\right] \xrightarrow[m_h t \gg 1]{} A_0\, t^{-3/4}\cos\left(m_h t + \theta_0\right), \tag{37}$$

where the asymptotic $t^{-3/4}$ envelope combines the explicit $t^{-1/4}$ prefactor with the $t^{-1/2}$ large-argument decay of $J_{1/4}, Y_{1/4}$.

This describes damped coherent oscillations of the Higgs-like field about its true vacuum, valid once the field is heavy compared to the expansion rate, $m_h t \gg 1$. Since $\dot{\delta\varphi} \propto t^{-3/4}\sin(m_h t + \theta_0)$ to leading order in this limit, the associated energy density $\rho_\varphi \sim \frac{1}{2}\dot{\varphi}^2$ redshifts as $t^{-3/2} \propto a^{-3}$, i.e. the oscillating scalar reduces like non-relativistic matter – consistent with standard coherent-oscillation/preheating behaviour for a massive scalar.
Now, using $\varphi \approx v$, $F \approx F_*$ in Eq. (11), we get

$$KT(t) \approx \frac{|\xi| v A_0 m_h}{4\pi F_*}\, t^{-3/4}\left|\sin(m_h t + \theta_0)\right|, \tag{38}$$

i.e. KT oscillates/rings in decaying bursts rather than relaxing to zero(monotonically).

4.4 Pre-transition roll-down near the symmetric point

Near the unstable extreme $\varphi \simeq 0$, $U_{,\varphi\varphi}(0) = -\lambda v^2 \equiv -m_s^2$, with $m_s^2 = \lambda v^2 = m_h^2/2$. In the same spectator/$R \simeq 0$ approximation as above, Eq. (25) linearizes to

$$\ddot{\varphi} + \frac{3}{2t}\dot{\varphi} - m_s^2\varphi \simeq 0, \tag{39}$$

which is the same equation as Eq. (35) with $m_h^2 \to -m_s^2$. The same substitution $\varphi = t^{-1/4}u(t)$ now produces a modified Bessel equation of order 1/4, so

$$\varphi(t) = t^{-1/4}\left[C_1 I_{1/4}(m_s t) + C_2 K_{1/4}(m_s t)\right] \xrightarrow[m_s t \gg 1]{} \frac{C_1}{\sqrt{2\pi m_s}}\, t^{-3/4} e^{m_s t}, \tag{40}$$

i.e. an exponentially growing diverging from $\varphi = 0$ toward $\pm v$, which gets cuts off once $|\varphi| \sim v$ where the linearization breaks down and the field matches onto the oscillatory solution of Eq. (37). This growing branch is the field-space analogue of the electroweak phase transition, and it is the source of KT burst expected of in a phase-transition-type model.

4.5 Adiabatic tracking solution in the presence of a small trace anomaly

for the radiation-era analysis, we shall consider the case where plasma departs slightly from an exactly conformal fluid, $\Delta \equiv 1 - 3w \in [0.01, 0.1]$, and keep U_0 general. Suppose the field is heavy compared to H ($m_h \gg H$), so that it tracks the instantaneous minimum of the effective potential

$$U_{\text{eff}}(\varphi; t) = U(\varphi) - \frac{1}{2}\xi R(t)\,\varphi^2, \tag{41}$$

its stationary condition $U_{\text{eff},\varphi} = 0$ will reproduce the quasi-static limit Eq. (25), $U_{,\varphi}(\varphi) = \xi R \varphi$. If we consider the nontrivial branch, we get

$$\varphi_*^2(t) = v^2 + \frac{\xi R(t)}{\lambda} \qquad \Longrightarrow \qquad \varphi_*(t) \approx v + \frac{\xi R(t)}{2\lambda v} \qquad \left(\left| \frac{\xi R}{\lambda v^2} \right| \ll 1 \right). \tag{42}$$

To get the system's leading order, let's evaluate the trace equation (26) with $\varphi \approx v$ at rest ($\dot{\varphi}, \ddot{\varphi} \to 0$) and $U(v) = U_0$:

$$R(t) \approx \frac{\Delta \rho_m(t) + 4U_0}{F_*}, \qquad F_* = M_0^2 + \xi v^2. \tag{43}$$

Provided $U_0 \ll \rho_m(t)$ (to make sure residual vacuum energy does not dominate the background, which we will check too), the leading-order Friedmann equation gives the ordinary radiation-domination scaling $\rho_m(t) \approx 3F_*/(4t^2)$ with $H = 1/(2t)$, so

$$R(t) \approx \frac{3\Delta}{4t^2} + \frac{4U_0}{F_*}. \tag{44}$$

The constant thing due to U_0 behaves like a tiny effective cosmological constant and does not drive $\dot{\varphi}_*$; only the matter-trace piece does.
Now, after differentiating Eq. (42), we get,

$$\dot{\varphi}_*(t) \approx \frac{\xi \dot{R}(t)}{2\lambda v} \approx -\frac{3\xi\Delta}{4\lambda v\, t^3}, \tag{45}$$

substituting $\varphi \approx v$, $F \approx F_*$ into Eq. (11) gives the closed-form adiabatic-tracking result

$$\boxed{KT(t) \approx \frac{3\xi^2\Delta}{16\pi\lambda F_*\, t^3}.} \tag{46}$$

This is the direct scalar-tensor analogue of the "active plasma era" tracking attractor found in the exponential-gravity project, and it is the regime most directly usable for a realistic radiation-era baryogenesis estimate (which we shall perform in Task 3), since it holds throughout radiation domination rather than only in a narrow transition window. Its validity requires heavy-field/adiabatic condition $m_h t \gg 1$, small-perturbation condition $|\xi R/(\lambda v^2)| \ll 1$, and (iii) $U_0 \ll \rho_m(t)$ such that the background stays radiation-dominated; these three inequalities define the window of cosmic time over which Eq. (46) is valid.

4.6 Dimensionless first-order autonomous system

The analytical branches above are controlled approximations. Lets cast the full system of Sec. **??**'s box into an autonomous first-order form in the number of e-folds $N \equiv \ln a$, with $' \equiv d/dN = H^{-1}d/dt$. This form is integrated numerically in Task 3–5.

Dimensionless variables. Normalizing all dynamical quantities to a fixed reference scale $M_{\rm Pl}$ (not dynamical F to make sure that the phase space stays smooth even where F or $\dot\varphi$ pass through zero), we define

$$u \equiv \frac{\varphi}{M_{\rm Pl}}, \qquad x \equiv \frac{\dot\varphi}{\sqrt{6}\,H M_{\rm Pl}}, \qquad \Omega_m \equiv \frac{\rho_m}{3H^2M_{\rm Pl}^2}, \tag{47}$$

together with two variables that track the fixed couplings λ, U_0 relative to the instantaneously evolving Hubble scale,

$$\Lambda \equiv \frac{\lambda M_{\rm Pl}^2}{H^2}, \qquad \Omega_{U_0} \equiv \frac{U_0}{3H^2M_{\rm Pl}^2}, \qquad \bar v \equiv \frac{v}{M_{\rm Pl}} \quad \text{(constant)}. \tag{48}$$

The dimensionless non-minimal coupling function and its logarithmic velocity are then purely algebraic in (u, x):

$$f(u) \equiv \frac{F}{M_{\rm Pl}^2} = m_0^2 + \xi u^2, \qquad m_0^2 \equiv \frac{M_0^2}{M_{\rm Pl}^2}, \qquad z \equiv \frac{\dot F}{FH} = \frac{2\sqrt{6}\,\xi u x}{f}, \tag{49}$$

so that $KT = |z|H/(8\pi)$, and the potential fraction is

$$y^2 \equiv \frac{U}{3H^2M_{\rm Pl}^2} = \frac{\Lambda}{12}\left(u^2 - \bar v^2\right)^2 + \Omega_{U_0}. \tag{50}$$

Dividing the Friedmann constraint (20) by $3H^2M_{\rm Pl}^2$ gives the algebraic closure relation

$$\boxed{\Omega_m = f(1+z) - x^2 - y^2} \qquad \Longleftrightarrow \qquad \Omega_\varphi \equiv 1 - \Omega_m = x^2 + y^2 - fz + (1-f). \tag{51}$$

Closing the system: $\dot H$ and $\ddot\varphi$. Unlike metric $f(R)$ gravity, where R itself is the propagating scalar, here φ is the propagating field and H is not independent.Both $\dot H$ and $\ddot\varphi$ must be solved simultaneously from the acceleration equation (24) and the scalar equation (25), since each contains both unknowns (via $\ddot F = 2\xi\dot\varphi^2 + 2\xi\varphi\ddot\varphi$ and via $R = 6(\dot H + 2H^2)$). Writing both equations as a linear system in $(\dot H, \ddot\varphi)$,

$$\begin{pmatrix} -2F & -2\xi\varphi \\ -6\xi\varphi & 1 \end{pmatrix}\begin{pmatrix} \dot H \\ \ddot\varphi \end{pmatrix} = \begin{pmatrix} \rho_m + p_m + (1+2\xi)\dot\varphi^2 - H\dot F \\ -3H\dot\varphi - \lambda\varphi(\varphi^2 - v^2) + 12\xi\varphi H^2 \end{pmatrix}, \tag{52}$$

with determinant

$$D = -2F - 12\xi^2\varphi^2 = -2\left(F + 6\xi^2\varphi^2\right) = -\left(2F + 3F_{,\varphi}^2\right), \tag{53}$$

using $F_{,\varphi} = 2\xi\varphi$. Equation (53) is actually (minus) the no-ghost combination $2KF + 3F_{,\varphi}^2$ of Condition 2 above ($K = 1$): the same quantity that must stay positive for a good scalar degree of freedom is, here, the determinant whose vanishing would make the closure of the numerical system singular. This acts like a cross-check that Condition 2 is not just a positivity requirement but the literal invertibility condition of the background dynamics.

Defining $\tilde{D} \equiv D/M_{\rm Pl}^2 = -2\left(f + 6\xi^2 u^2\right)$ and the dimensionless source combinations

$$G_A \equiv 3\Omega_m(1+w) + 6(1+2\xi)x^2 - fz, \tag{54}$$

$$G_B \equiv -3\sqrt{6}\,x - \Lambda u\left(u^2 - \bar{v}^2\right) + 12\xi u, \tag{55}$$

Cramer's rule applied to Eq. (52) gives the closed, dimensionless expressions

$$q \equiv \frac{\dot{H}}{H^2} = \frac{G_A + 2\xi u\, G_B}{\tilde{D}}, \qquad \frac{\ddot{\varphi}}{H^2 M_{\rm Pl}} = \frac{-2fG_B + 6\xi u\, G_A}{\tilde{D}}. \tag{56}$$

The autonomous system. Using $u' = \sqrt{6}x$ and $x' = \ddot{\varphi}/(\sqrt{6}H^2 M_{\rm Pl}) - xq$, the full closed system in e-folds is

$$\boxed{u' = \sqrt{6}\,x,\ x' \qquad = \frac{(6\xi u - x)\,G_A - 2\,(f + \xi u x)\,G_B}{ildeD},\ \Lambda' = -2\Lambda q,\ \Omega_{U_0}' \qquad = -2\Omega_{U_0}\,q.} \tag{57}$$

,with $f, z, y^2, \Omega_m, G_A, G_B, \tilde{D}, q$ all algebraic functions of $(u, x, \Lambda, \Omega_{U_0})$ as defined above, and $w = w(N)$ (constant $w = 1/3$ for exact radiation, or $w = (1-\Delta)/3$ with a prescribed trace-anomaly profile $\Delta(N)$ during a threshold window). This is the four-dimensional (plus Ω_m-constraint) autonomous system to be evolved numerically in Task 3–5.

Radiation-era numerical consistency check. Since every numerical trajectory must be checked against $\Omega_\varphi \ll 1$ (subdominant scalar fraction) and against the exact algebraic constraint $\Omega_m + x^2 + y^2 - fz = f$ being satisfied to high precision at every step; the size of the residual is the direct numerical analogue of the Friedmann-constraint monitoring recommended for the exponential-gravity as I know. In the regime $m_h \gg H$, $\Omega_\varphi \ll 1$, this system must reproduce, as an attractor, the closed-form adiabatic-tracking result of Eq. (46); this reproduction is itself the recommended analytical-versus-numerical cross-check for this branch.

4.7 Summary matrix

Regime	Condition/Ansatz	Direct solution	Classification
Global/Universal	Arbitrary $\varphi(t)$, $a(t)$	None (not generally solvable)	Blocked by cubic nonlinearity + two-way φ–R feedback
GR-like vacuum	$\varphi = \pm v$, $\dot{\varphi} = 0$, $R = 0$, $U_0 = 0$	$\varphi = \text{const}$, $F = F_*$, $KT = 0$	Exact fixed point (sterile)
Symmetric point	$\varphi = 0$, $\dot{\varphi} = 0$, $R = 0$	$\varphi = 0$	Exact but unstable fixed point
Post-transition oscillation	$\varphi = v + \delta\varphi$, $R \simeq 0$ (spectator)	$\delta\varphi = t^{-1/4}[C_1 J_{1/4}(m_h t) + C_2 Y_{1/4}(m_h t)]$	Exact linear solution (Bessel, damped oscillatory)
Pre-transition roll	$\varphi \simeq 0$, $R \simeq 0$ (spectator)	$\varphi = t^{-1/4}[C_1 I_{1/4}(m_s t) + C_2 K_{1/4}(m_s t)]$	Exact linear solution (modified Bessel, growing)
Active plasma era	$m_h \gg H$, $\Delta \neq 0$ small, U_0 subdominant	$\varphi_* \approx v + \xi R/(2\lambda v)$, $KT \propto t^{-3}$	Algebraic adiabatic attractor (primary baryogenesis driver)

4.8 Analytical verdict

As in the exponential-gravity project, no single formula solves this model across all cosmic epochs, but the radiation era decomposes cleanly into a small number of controlled regions: an exact sterile GR fixed point, an unstable symmetric point whose decay is described exactly by modified Bessel functions, a damped oscillatory regime about the true vacuum described by ordinary Bessel functions, and – for baryogenesis – an algebraic adiabatic tracking solution sourced by the small trace anomaly $\Delta = 1 - 3w$ that gives the closed-form power law $KT(t) \propto t^{-3}$ of Eq. (46). Together with the coupling choices $\mathcal{I}(\varphi) = \varphi^2/M_{\text{Pl}}$ or $\mathcal{I}(\varphi) = M_{\text{Pl}}^2 \ln(F/M_{\text{Pl}}^2)$ from Sec. 2, these solutions provide the inputs $\dot{\varphi}(t)$ (or $\dot{F}(t)$) needed to evaluate the equilibrium $B - L$ yield and the freeze-out asymmetry n_b/s to be performed in Task 3.

5 Task 3: Baryon Asymmetry for the Linear and Logarithmic Couplings

I will be following this chai for task 3,

$$\{F, K, U\} \longrightarrow \{H(t), \varphi(t)\} \longrightarrow KT(t) = \frac{|\dot{F}|}{8\pi F} \longrightarrow \dot{\mathcal{I}}(t) \longrightarrow \mu_{B-L}(t) \xrightarrow[\Gamma_{B-L}(T_D)=H(T_D)]{} \left.\frac{n_B}{s}\right|_{T_D}. \tag{58}$$

The gravitational sector $(H(t), \varphi(t), KT(t))$ was already fully determined in previous tasks(1&2), this section will give the remaining particle-physics links.

5.1 Two couplings to study

As fixed in Sec. 2, we evaluate the asymmetry for

$$\mathcal{I}_{\rm lin}(\varphi) = \varphi, \qquad \dot{\mathcal{I}}_{\rm lin} = \dot\varphi, \qquad d_{\rm lin} = 1, \tag{59}$$

$$\mathcal{I}_{\rm log}(\varphi) = M_{\rm Pl}^2 \ln\left(\frac{F}{M_{\rm Pl}^2}\right), \qquad \dot{\mathcal{I}}_{\rm log} = M_{\rm Pl}^2 \frac{\dot F}{F} = 8\pi M_{\rm Pl}^2 \epsilon_F\, KT, \qquad d_{\rm log} = 2, \tag{60}$$

with $\mu_{B-L} = c_{\rm STB}\dot{\mathcal{I}}/M_*^d$ in both cases (Sec. 1). The two are physically different objects: $\mathcal{I}_{\rm log}$ is, by construction, an *exact* multiple of KT at every instant, while $\mathcal{I}_{\rm lin}$ tracks the scalar velocity, which is related to KT only through the model- and field-dependent ratio (from the "natural case" identity of Sec. 1)

$$\dot{\mathcal{I}}_{\rm lin} = \dot\varphi = \epsilon_\varphi \frac{4\pi F}{|\xi|\varphi} KT, \qquad \epsilon_\varphi \equiv {\rm sign}(\dot\varphi). \tag{61}$$

Because $F/(|\xi|\varphi)$ is not constant, $\mathcal{I}_{\rm lin}$ and $\mathcal{I}_{\rm log}$ need not peak at the same instant along a given trajectory, even though both ultimately derive from the same $F(\varphi)$.

5.2 Evaluating the sources on the adiabatic-tracking background

Of the branches found in Task 2, only the adiabatic-tracking solution (Sec. 4.5) is active throughout the whole radiation era rather than only in a narrow transition window, so it is the natural background on which to evaluate a freeze-out asymmetry (the transient oscillation/roll branches are revisited briefly in Sec. 5.6). On this background, $\varphi \approx v$, $F \approx F_* = M_0^2 + \xi v^2$, and, from Eqs. (42)–(46),

$$\dot{\mathcal{I}}_{\rm lin}(t) \approx \dot\varphi_*(t) \approx -\frac{3\xi\Delta}{4\lambda v\, t^3}, \qquad \dot{\mathcal{I}}_{\rm log}(t) \approx 8\pi M_{\rm Pl}^2 \epsilon_F\, KT(t) \approx \epsilon_F \frac{3\xi^2 \Delta M_{\rm Pl}^2}{2\lambda F_*\, t^3}. \tag{62}$$

On this branch $\xi > 0$, $\varphi > 0$ and $\Delta > 0$ give $\dot\varphi_* < 0$, so $\epsilon_\varphi = \epsilon_F = -1$ identically. the two couplings predict the same sign for μ_{B-L} here (refer to Sec. 5.8 for when this need not hold).

5.3 Freeze-out evaluation

Task 3 requires an explicit decoupling temperature T_D, fixed by some microscopic $B-L$-violating process with rate $\Gamma_{B-L}(T)$, via $\Gamma_{B-L}(T_D) = H(T_D)$. This process belongs to the particle-physics sector and is logically independent of the scalar-tensor gravity sector: the latter only supplies the source $\dot{\mathcal{I}}(T_D)$ to be evaluated *at* T_D. Let's follow the dimension-five Weinberg operator, with

$$\Gamma_W(T) = \frac{3}{4\pi^3}\frac{\bar m_\nu^2}{v_H^4} T^3, \qquad H(T) = \sqrt{\frac{\pi^2 g_*}{90}}\frac{T^2}{M_{\rm Pl}}, \tag{63}$$

which gives [3]

$$\boxed{T_D = \frac{4\pi^3}{3}\sqrt{\frac{\pi^2 g_*}{90}}\frac{v_H^4}{\bar m_\nu^2 M_{\rm Pl}}.} \tag{64}$$

With $v_H = 246$ GeV, $\bar m_\nu \simeq 0.05$ eV (atmospheric-scale benchmark), $g_* = 106.75$, and $M_{\rm Pl} = 2.435 \times 10^{18}$ GeV,

$$T_D \approx 8.5 \times 10^{13}\ \text{GeV}. \tag{65}$$

[3] I have re-derived this directly from $\Gamma_W(T_D) = H(T_D)$, since the pdf shared has prefactor omiting a factor of π^2

Any other completion (e.g. a different dimension-five operator, or explicit right-handed neutrinos[4]) would simply replace T_D with a different number without changing the structure below. the sensitivity of final asymmetry to T_D is made explicit in Eq. (67)–(68).

Following the standard thermal chain (relativistic species with degeneracy $\hat{g}_{B-L} \equiv \sum_i g_i q_i^2$, entropy density $s = \frac{2\pi^2}{45} g_{*s} T^3$, and a sphaleron conversion factor $c_{\rm sph} = 28/79$ for the Standard Model field content),

$$\left.\frac{n_B}{s}\right|_{T_D} \equiv Y_B \simeq c_{\rm sph} \frac{15\hat{g}_{B-L}}{4\pi^2 g_{*s}} \frac{\mu_{B-L}(T_D)}{T_D}. \tag{66}$$

5.4 Closed-form results

Converting the time-domain sources (62) to temperature using $3F_* H^2 \approx \rho_r = \frac{\pi^2}{30} g_* T^4$ (leading order, spectator condition) gives $t(T) = \sqrt{45F_*/(2\pi^2 g_*)}\, T^{-2}$, and hence $t^{-3} = (2\pi^2 g_*/45F_*)^{3/2} T^6$. Putting $F_* \equiv M_{\rm Pl}^2$ (the vacuum value of F is, by definition, the observed effective Planck mass), substitution into Eq. (66) will give us

$$Y_B^{\rm log}(T_D) \approx \frac{90\, \hat{g}_{B-L} c_{\rm sph} c_{\rm STB}\, \xi^2 \Delta\, \epsilon_F}{16\pi^2 g_{*s} \lambda} \left(\frac{2\pi^2 g_*}{45}\right)^{3/2} \frac{T_D^5}{M_*^2 M_{\rm Pl}^3}, \tag{67}$$

$$Y_B^{\rm lin}(T_D) \approx -\frac{45\, \hat{g}_{B-L} c_{\rm sph} c_{\rm STB}\, \xi \Delta\, \epsilon_\varphi}{16\pi^2 g_{*s} \lambda\, v} \left(\frac{2\pi^2 g_*}{45}\right)^{3/2} \frac{T_D^5}{M_* M_{\rm Pl}^3}. \tag{68}$$

Both scale as T_D^5 which is a strong sensitivity to the decoupling scale, inherited from $KT \propto t^{-3} \propto T^6$ scaling of the tracking branch divided by the one explicit power of T_D in Eq. (66).
Interestingly,the two formulas differ in three structural ways: the power of ξ (ξ^2 vs. ξ^1, tracing back to $\dot{\mathcal{I}}_{\rm log} \propto KT \propto \xi^2$ against $\dot{\mathcal{I}}_{\rm lin} = \dot{\varphi} \propto \xi$), the power of M_* ($d = 2$ vs. $d = 1$), and an explicit inverse power of v present only in linear case.

5.5 An numerical example and representative points

To ground Eqs. (67)–(68) we adopt the following explicitly stated values: $g_* = g_{*s} = 106.75$, $\hat{g}_{B-L} = 100$ (order-of-magnitude, summed over relativistic $B-L$-charged species), $c_{\rm STB} = 1$, $\Delta = 0.05$ (mid-point of the given range $[0.01, 0.1]$), $\lambda = 0.13$, $U_0 = 0$, and the pure induced-gravity closure $M_0 = 0$, so that $F_* = \xi v^2 = M_{\rm Pl}^2 \Rightarrow v = M_{\rm Pl}/\sqrt{\xi}$ (this removes one free parameter and ties the vacuum scale directly to ξ).
We choose to adopt the success band

$$0.5 < \frac{|Y_B|}{8.8 \times 10^{-11}} < 2. \tag{69}$$

Given table 1 lists, for representative values of ξ, the cutoff scale M_* required by each coupling to land exactly on the target $Y_B = 8.8 \times 10^{-11}$, together with M_*/T_D (the EFT-validity ratio discussed in Sec. 5.7). We can see, for the logarithmic coupling, $\xi = 1$ is an excluded point ($M_* < T_D$), $\xi \gtrsim 9.4$ is the boundary of viability, and $\xi = 10, 10^2, 10^3, 10^4$ are all possible/successful points. For the linear coupling, every row up to $\xi = 10^4$ is excluded ($M_* < T_D$ in every case shown); viabile only after $\xi \gtrsim 2.9 \times 10^4$ (derived in Sec. 5.7), i.e. beyond the conventional Higgs-inflation range $\xi \lesssim 10^4$ foretold in Task 1. An quantitative example of the comparison is performed in Sec. 5.8.

[4] Wink!

ξ	v [GeV]	$M_*^{\log}$ [GeV]	$M_*^{\log}/T_D$	$M_*^{\rm lin}$ [GeV]	$M_*^{\rm lin}/T_D$
1	2.4×10^{18}	9.1×10^{12}	0.11	1.7×10^{7}	2.0×10^{-7}
10	7.7×10^{17}	9.1×10^{13}	1.06	5.3×10^{8}	6.3×10^{-6}
10^2	2.4×10^{17}	9.1×10^{14}	10.6	1.7×10^{10}	2.0×10^{-4}
10^3	7.7×10^{16}	9.1×10^{15}	106	5.3×10^{11}	6.3×10^{-3}
10^4	2.4×10^{16}	9.1×10^{16}	1.06×10^{3}	1.7×10^{13}	0.20
10^5	7.7×10^{15}	9.1×10^{17}	1.06×10^{4}	5.3×10^{14}	6.3

Table 1: Cutoff scale M_* required to reproduce $Y_B = 8.8 \times 10^{-11}$ exactly, for the fiducial parameters of Sec. 5.5 and $T_D \approx 8.5 \times 10^{13}$ GeV. Rows with $M_*/T_D < 1$ (boldface criterion, Sec. 5.7) fail the EFT-validity test and are thus not included (not successful, points)

5.6 Parameter inference

On the tracking branch used above:

- **Magnitude of the source.** Controlled by ξ, Δ, λ, v (or, equivalently, M_*), and by T_D through the steep T_D^5 scaling of Eqs. (67)–(68).
- **Timing.** The tracking source is monotonic, $KT \propto t^{-3} \propto T^6$. it is largest at the highest-temperature end of its validity window and simply decreases after. Also, no peak to locate, qualitatively different from the transient branches: the pre-transition roll (Sec. 2.4) grows until $|\varphi| \sim v$ and then matches on to the post-transition oscillation (Sec. 2.3), whose KT rings in decaying bursts with period $\sim 2\pi/m_h$ (Eq. (37)). A decoupling temperature that happens to coincide with one of these bursts, rather than with the smooth tracking background, could enhance or, depending on the phase θ_0, suppress the instantaneous source relative to the tracking estimate used here. for a full treatment of this possibility, we req numerical system of Sec. 4.6 and is Task 5.
- **Sign.** Fixed by sign(Δ), ξ, and φ's branch (Sec. 5.8); for $\Delta > 0$, $\xi > 0$, $\varphi \approx +v$, both couplings give $Y_B < 0$ for our sign convention (flippable by the sign of $c_{\rm STB}$, which is an independent Wilson coefficient for each of the two, physically distinct, effective operators).
- **Duration.** The tracking source stays active throughout radiation domination, subject only to the validity window identified in Task 2 (heavy-field, small-perturbation, U_0-subdominance); the transient branches are active only for a Hubble time or so around the relevant threshold/transition.
- **Position of T_D relative to the background phase.** Our worked example assumes T_D falls during the smooth tracking phase, not during a sharp threshold kick. It was verified in Task 2 (the heavy-field and small-perturbation ratios were $\sim 10^{-6}$ and $\sim 10^{-9}$ respectively at T_D for $\xi = 10^4$), so the assumption is justified for the parameters used here.

5.7 Viability tests

- **EFT validity ($M_* \gtrsim T_D$).** This is the binding constraint in Table 1. Solving $M_*^{\log}(\xi) = T_D$ and $M_*^{\rm lin}(\xi) = T_D$ for ξ (using the scalings $M_*^{\log} \propto \xi$, $M_*^{\rm lin} \propto \xi^{3/2}$ that follow from Eqs. (67)–(68) with $v = M_{\rm Pl}/\sqrt{\xi}$) gives the minimum viable non-minimal coupling for each case, for our parameters:

$$\xi_{\min}^{\log} \approx 9.4, \qquad \xi_{\min}^{\mathrm{lin}} \approx 2.9 \times 10^4. \tag{70}$$

- **Chemical potential small compared to T.** At the targeted asymmetry which is around $\mu_{B-L}/T \sim 4\pi^2 g_{*s} Y_B/(15\hat{g}_{B-L}) \approx 2.5 \times 10^{-10} \ll 1$ for both couplings (the equilibrium thermal-integral expansion used to derive Eq. (66) is actually self-consistent).

- **Operator does not dominate the scalar/gravitational equations.** The baryogenesis operator contributes a force $\sim c_{\mathrm{STB}} n_{B-L}/M_*^d$ to the scalar equation of motion, to be compared with the quartic force $\sim \lambda v^3$ already present in Eq. (25); since $n_{B-L} = Y_B s \sim 10^{-11} s$ is parametrically tiny, this ratio is generically negligible whenever the EFT-validity bound above is satisfied, so backreaction on the background derived in Tasks 1–2 is unintended and safely absent.

- **Background remains inside the Task 2 validity window.** As verified in Sec. 5.6 (heavy-field and small-perturbation ratios both $\ll 1$ at T_D).

- **Model stability ($F > 0$, no ghost).** Guaranteed for all $\xi > 0$ by Task 1, Sec. 3.10, independent of the baryogenesis parameters.

- **G_{eff} does not cross zero.** Same condition as above.

- **T_D lies within a physical epoch.** $T_D \approx 8.5 \times 10^{13}$ GeV is far above BBN (~ 1 MeV) and below M_{Pl}; it requires only that reheating occurred at or above this scale, an implicit assumption of any high-scale baryogenesis scenario.

- **Γ_{B-L} possibly in equilibrium before T_D.** Since $\Gamma_W/H \propto T$ for the Weinberg operator, $\Gamma_W \gg H$ automatically at all $T > T_D$, so the process is in equilibrium at early times and freezes out exactly at T_D by construction.

Only parameter points simultaneously satisfying all of the above in particular Eq. (70) should be counted as successful; points with the correct numerical value of Y_B but $M_* < T_D$ are excluded, not successful, exactly as thought and told/given/

5.8 Comparison of linear and logarithmic couplings

- **reaching the observed asymmetry more naturally:** At fixed $M_* = M_{\mathrm{Pl}}$, the logarithmic coupling needs only $\xi \approx 2.7 \times 10^5$ times less enhancement than the linear one to reach the same $|Y_B|$ (compare the ξ^2 vs. $\xi^{3/2}$ scalings, further amplified here by $v = M_{\mathrm{Pl}}/\sqrt{\xi}$ shrinking as ξ grows, which suppresses $\dot{\mathcal{I}}_{\mathrm{lin}} \propto 1/v$ less than it helps KT). At fixed[5], $\xi \sim 1$–10^4, the logarithmic coupling is viable while the linear one is not (Eq. (70)): the logarithmic coupling reaches the target more naturally.

- **lower suppression scale:** At fixed ξ, the linear coupling needs a much **lower** M_* than the logarithmic one (Table 1: e.g. at $\xi = 10^4$, $M_*^{\mathrm{lin}} \approx 1.7{\times}10^{13}$ GeV versus $M_*^{\log} \approx 9.1{\times}10^{16}$ GeV) the opposite ordering from the previous bullet. Thus, the answer is scan-dependent rather than a singlular verdict.

[5]taking natural one

- **Sensitivity to initial conditions.** Neither of them seem sensitive to initial conditions *on the tracking branch*, since it is a quasi-static attractor (Sec. 4.5) that forgets its initial info. On the transient oscillation/roll branches, both couplings inherit the same amplitude/phase dependence (A_0, θ_0) from the same $\delta\varphi(t)$, so neither is more IC-sensitive than the other there.

- **Correlation with KT.** The logarithmic coupling is actually exactly proportional to KT at every instant (Sec. 1); the linear coupling is proportional to KT only up to the field-dependent ratio $F/(|\xi|\varphi)$ of Eq. (61), which varies along the trajectory.

- **Same sign:** On the branch used throughout this section ($\varphi \approx +v$, $\xi > 0$), it turns out to be true as both are governed by $\epsilon_F = \epsilon_\varphi$. Though, on the mirror branch $\varphi \approx -v$, $\dot{\mathcal{I}}_{\rm lin} = \dot{\varphi}$ flips sign with φ alone, while $\dot{\mathcal{I}}_{\rm log} \propto \dot{F} = 2\xi\varphi\dot{\varphi}$ depends on the *product* $\varphi\dot{\varphi}$, the two couplings can therefore disagree in relative sign between the two vacuums, a differentiating feature not visible on a single branch.

- **Cooling vs. heating at decoupling.** This requires the sign of $(\dot{KT})$ from the Riccati equation of Eq. (30) (Task 4)[6]. we only note here that both couplings use the *same* background $KT(t)$, so whichever sign $(\dot{KT})(T_D)$ turns out to have applies to both couplings' decoupling points simultaneously on the tracking branch.

- **Behaviour near the symmetric point $\varphi = 0$.** Exactly at $\varphi = 0$, $F_{,\varphi} = 2\xi\varphi = 0$ so $KT = 0$ identically, and therefore $\dot{\mathcal{I}}_{\rm log} = 0$ there as well . the logarithmic source is in a way killed at the symmetric point, in the same way it is suppressed near a least-coupling point in the Green-group dilaton models. The linear source, $\dot{\mathcal{I}}_{\rm lin} = \dot{\varphi}$, is generically *nonzero* at $\varphi = 0$ during the pre-transition roll (Eq. (40), where $\dot{\varphi} \propto e^{m_s t} \neq 0$ even as $\varphi \to 0$): the linear coupling remains active precisely where the logarithmic coupling (and KT itself) vanishes.

5.9 Numerical part

[7] For the upcoming numerical things for Task 5, both sources are already algebraic functions of the dimensionless variables (u, x) of Sec. 4.6: $\dot{\mathcal{I}}_{\rm lin} = \sqrt{6}\, xHM_{\rm Pl}$ and $\dot{\mathcal{I}}_{\rm log} = M_{\rm Pl}^2 Hz$ (with z as defined there), so $\mu_{B-L}(N)$ and thus, $Y_B(N)$ can be evaluated at every e-fold step of the integration without any additional things. only freeze-out condition $\Gamma_{B-L}(T(N)) = H(T(N))$ needs to be located along the numerically integrated trajectory.

[6] To be done

[7] leading to Task 5

5.10 Figures

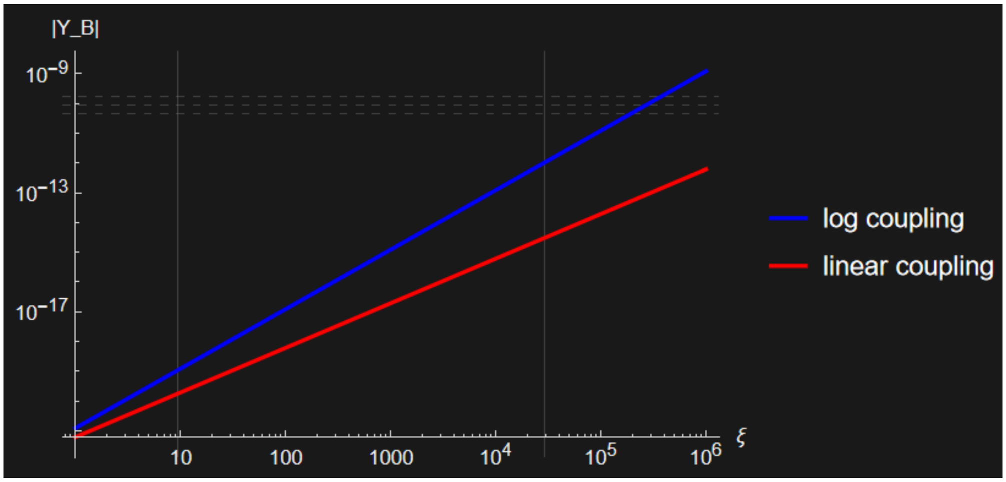

Figure 1: Baryon asymmetry vs. non-minimal coupling ξ for both couplings, with the EFT-viability cutoffs marked.

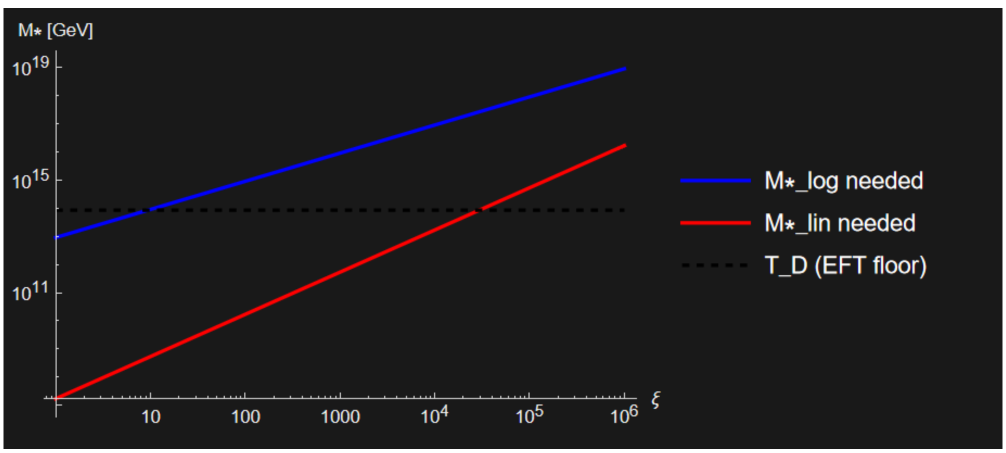

Figure 2: Required cutoff scale vs. ξ for both couplings, with the EFT-validity floor.

5.11 Summary of Task 3

Using the adiabatic-tracking background of Task 2, both the linear ($\mathcal{I} = \varphi$) and logarithmic ($\mathcal{I} = M_{\rm Pl}^2 \ln(F/M_{\rm Pl}^2)$) baryogenesis couplings admit closed-form expressions, Eqs. (67)–(68), for the freeze-out asymmetry n_B/s in terms of the model parameters $(\xi, \lambda, v, \Delta)$, the cutoff M_*, and the decoupling temperature T_D. Both can reproduce the observed $Y_B \approx 8.8 \times 10^{-11}$ for viable choices of parameters, but the two couplings occupy genuinely different corners of parameter space: the logarithmic coupling is viable already for $\xi \gtrsim 9$ (very much inside the Higgs-inflation range), while the linear coupling requires $\xi \gtrsim 3 \times 10^4$ (beyond the conventional range) for the same choices, and requires a systematically lower cutoff M_* at any fixed ξ. The two couplings are exactly degenerate with KT only in the logarithmic case, and only the linear coupling remains active at the symmetric point $\varphi = 0$. These closed-form results and the placeholder figures above set up the sign/root analysis of $(\dot{KT})$ (Task 4) and the combined parameter-space maps (Task 5).

6 Task 4:

References

1. F. L. Bezrukov and M. Shaposhnikov, “The Standard Model Higgs boson as the inflaton,” arXiv:0710.3755.

2. M. Ballardini, F. Finelli, C. Umiltà and D. Paoletti, “Cosmological constraints on induced gravity dark energy models,” arXiv:1601.03387.

3. M. Ballardini, “Cosmological constraints on the gravitational constant,” arXiv:2111.09168.

4. M. Karčiauskas and J. J. Terente Díaz, “Slow-Roll Inflation in the Jordan Frame,” arXiv:2206.08677.

5. C. van de Bruck and C. Longden, “Higgs Inflation with a Gauss-Bonnet term in the Jordan Frame,” arXiv:1512.04768.

6. V. Faraoni and A. Giusti, “Thermodynamics of scalar-tensor gravity,” arXiv:2103.05389.

7. S. Giardino, V. Faraoni and A. Giusti, “First-order thermodynamics of scalar-tensor cosmology,” arXiv:2202.07393.

8. H. Davoudiasl, R. Kitano, G. D. Kribs, H. Murayama and P. J. Steinhardt, “Gravitational baryogenesis,” arXiv:hep-ph/0403019.

9. D. S. Pereira, “Scalar–tensor baryogenesis: a scalar–tensor completion of gravitational baryogenesis,” arXiv:2412.06984.

10. D. S. Pereira, B. A. Fernandes and J. P. Mimoso, “Gravitational baryogenesis beyond the spectator approximation,” arXiv:2603.11837.